Simulation of Image Defect at Edges of Images in Single Component Development Systems

J. Yoo, Jeanman Sur, Ki-Jae Do, and Jongmoon Eun; Digital Printing Division, Samsung Electronics Co., Ltd.; Suwon, Korea

Abstract

We perform numerical simulations of image defect at edges of solid images in non-contact single-component development systems using nonmagnetic toner. Line deletion at the leading edge of halftone images when the image is placed below a solid pattern often occurs in development systems in which the photoconductor drum surface and the development roller surface rotate in opposite directions in the development gap. This defect is examined by simulating development process in the region between the drum and the roller. The toner movement is traced by solving the equation of motions for toner particles. The Green function approach is used to calculate the electric field in the gap. An efficient numerical method is applied to integrate the Green function over charge distributions over the photoconductor with numerical stability.

Introduction

In single component development systems edges of solid images are one of the most frequent sources of image defects. This is because there is an abrupt change of the charge density on the photoconductor at the edges of solids so that electric field lines originating from one side near the edges on the surface of the photoconductor cannot connect the photoconductor and the electrode (or development roller) but bridge back to the other side of the edges on the photoconductor. Defects which often occur at edges are slow toner, line deletion, dark solid edges, etc [1, 2, 3, 4]. In this paper we are concerned with one such defect in a non-contact single component development system using non-magnetic toner where triboelectrifically charged toner particles jump between the photoconductor drum and the development roller for the development of images onto the drum. Though deleted lines occur at edges of a solid in many implementations of electrophotographic systems, they could appear wider at the leading edge of halftone images placed below the solid images (see Fig. 1) when the drum and the roller rotate in the same angular direction such that their surfaces move in opposite directions in the development gap.

We examine the image defect by simulating the toner movement in the gap in two dimensions. To trace toner particles the equation of motion is constructed with three force terms: electrostatic force, Stokes viscous force, and random force. To calculate the electric field between the drum and roller the Green function is found and is integrated over the charge distribution on the photoconductor. For those integrations a numerical method is developed which can give results of any accuracy with numerical stability.

Electric Field

The electric field between the photoconductor drum and the development roller for a non-contact development system will be calculated in a two dimensional geometry of the development gap. Photoconductor drums and development rollers are metallic cylinders coated with photoconductor and rubber, respectively. Here, the drum and the roller are assumed to be infinitely long cylinders, and the conformal transformation method will be used to find the electric field in the gap between the two infinitely long cylinders. The dielectric properties of the photoconductor will be ignored by using the dielectric thickness for the photoconducting layer, and similarly for the development roller. With a surface charge distribution on the photoconductor, the electric field in the gap can be obtained as a sum of a homogeneous solution and an inhomogeneous solution of the Poisson equation for the configuration. One can easily find the homogeneous solution [5, 6]. The Green function is first calculated and is integrated over the surface charge density on the drum to find the inhomogeneous solution.

As the drum and the roller are considered as two circles in complex z plane (see Fig. 2), the two circles can be conformally transformed into two concentric circles in complex t plane. The transformation can be represented as [5]

$$re^{i\theta} + c_t = \frac{1}{\rho e^{i\phi} + c_z}, \tag{1}$$

where ρ and ϕ are polar coordinates with respect to the center of the circle for the drum and real axis in z plane and c_z is the distance from the coordinate origin $z = 0$ to this center. r, θ and c_t are similarly defined with respect to the concentric center in t plane. With the two concentric cylinders one can find the Green

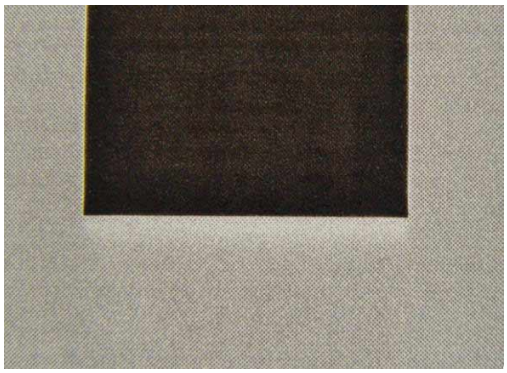

Figure 1. *A deleted line of about 1mm width at the leading edge of a halftone image below a black solid in a system in which the surfaces of the photoconductor drum and the development roller rotate in opposite directions in the development gap. The development proceeds from top to bottom.*

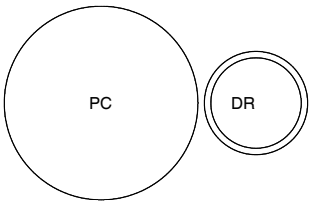

Figure 2. *The circles for the photoconductor drum and the development roller. The outer radii of the drum and the roller are* $30mm$ *and* $16mm$*, respectively, with a photoconductor layer of thickness* $21\mu m$ *on the drum and a rubber layer of* $1mm$ *on the roller. The dielectric thicknesses for the two layers are used in the calculations. The gap is* $200\mu m$*, which is exaggerated in the figure.*

function G for the region between the two cylinders in t plane,

$$G(r,r') = \frac{1}{2\pi \ln\frac{r_2}{r_1}} \ln\frac{r_1}{r_<} \ln\frac{r_>}{r_2} - \frac{1}{\pi}\sum_{m=1}^{\infty} \frac{1}{2m(r_2^{2m}-r_1^{2m})} \times (r_<^m - r_1^{2m} r_<^{-m})(r_>^m - r_2^{2m} r_>^{-m}) \cos\left[m(\theta-\theta')\right], \quad (2)$$

where the notational convention in Ref. [7] is used for $r_<$ and $r_>$, and r_1,r_2 are radii for the drum and the roller in t plane, respectively. The real Green function $G(r,r')$ can be analytically continued into the complex Green function $G(t,t')$ in t plane. The differentiation of $G(t,t')$ gives the electric field as a function of complex t: for $r < r'$

$$E(t,t') = \frac{1}{2\pi \ln\frac{r_2}{r_1}} \frac{-t^2}{t-c_t} \ln\frac{r'}{r_2} + \frac{1}{\pi}\sum_{m=1}^{\infty} \frac{m}{2m\left[1-(\frac{r_1}{r_2})^{2m}\right]} \frac{-t^2}{t-c_t} \times \left[\left(\frac{t-c_t}{r'e^{i\theta'}}\right)^m + \left(\frac{r_1^2}{(t-c)r'e^{-i\theta'}}\right)^m - \left(\frac{(t-c_t)r'e^{-i\theta'}}{r_2^2}\right)^m - \left(\frac{r_1^2 r'e^{i\theta}}{r_2^2(t-c_t)}\right)^m\right], \quad (3)$$

and for $r > r'$

$$E(t,t') = \frac{1}{2\pi \ln\frac{r_2}{r_1}} \frac{-t^2}{t-c_t} \ln\frac{r_1}{r'} + \frac{1}{\pi}\sum_{m=1}^{\infty} \frac{m}{2m\left[1-(\frac{r_1}{r_2})^{2m}\right]} \frac{-t^2}{t-c_t} \times \left[-\left(\frac{r'e^{i\theta}}{t-c_t}\right)^m + \left(\frac{r_1^2}{(t-c_t)r'e^{-i\theta'}}\right)^m - \left(\frac{(t-c_t)r'e^{-i\theta'}}{r_2^2}\right)^m + \left(\frac{r_1^2(t-c_t)}{r_2^2 r'e^{\theta'}}\right)^m\right]. \quad (4)$$

The electric field Eq. (3) and Eq. (4) from a single charged particle source have to be integrated over the surface charge density on the photoconductor to obtain the field for the charge density. This requires the integration of each term in Eq. (3) and (4) over the charge density with respect to coordinate ϕ with ρ fixed at the drum radius. When one assumes that the charge distribution consists of step functions only, these integrals result in the form,

$$I_m = \int_{\phi_1}^{\phi_2} C^m \left(A + \frac{1}{Re^{i\phi}+B}\right)^m d\phi\,, \quad (5)$$

where R is the radius of the photoconductor drum, and A, B, and C are complex constants. It can be shown that the integrals I_m in Eq. (5) satisfies a three-term recurrence relation,

$$I_m - \left(2A+\frac{1}{B}\right)I_{m-1} + A\left(A+\frac{1}{B}\right)I_{m-2} = -\frac{i}{(m-1)B}\left(A+\frac{1}{Re^{i\phi}+B}\right)^{m-1},\ m = 2,3,4,\cdots. \quad (6)$$

Using the recurrence relation Eq. (6), one can compute the integral Eq. (5). The recurrence relation can be either stable or unstable depending upon the relationships among A, B, and C [8]. For the stable cases, repetitive applications of the recurrence relation Eq. (6) give the integral Eq. (5). For the unstable cases, one can diagonalize the tridiagonal matrix constructed from the recurrence relation to obtain I_m, which is numerically stable. Thus, in either case the integral Eq. (5) can be computed with numerically stable methods, which allows one to evaluate Eq. (5) to any given accuracy. Using the methods described above we find the electric field for the development gap between the photoconductor drum and the development roller. Fig. 3,4,5 show electric potential and electric field lines obtained from this method.

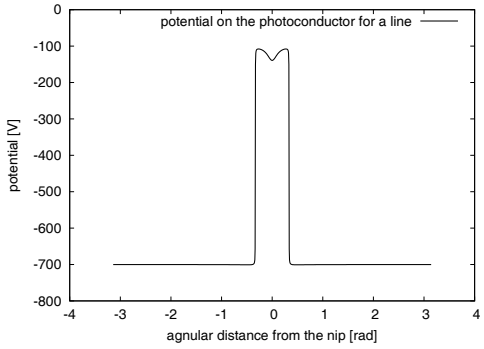

Figure 3. *Electric potential at* $5\mu m$ *from the drum for an image of a line of 10mm thickness on the photoconductor with the line center at the position of the smallest gap. The low and high potential areas on the photoconductor have the surface charge densities equivalent to -700V and -100V in infinitely extended free space, and the shaft of the development roller has the bias voltage of -1100V. 1000 data points are obtained from calculations to plot the graph.*

Equation of Motion

To simulate the movement of toner particles in the gap in the development process, one needs to model the force which acts on the toner particles. The force is due to many different sources with different nature of physics. The most dominant contribution comes from the electrostatic force from bias voltages of

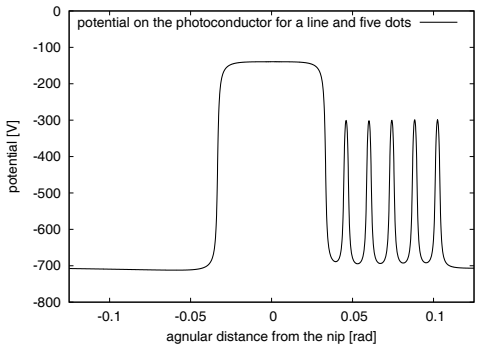

Figure 4. *Electric potential at $5\mu m$ from the drum for images of a line of 1mm thickness and five dots on the photoconductor with the line center at the position of the smallest gap. The same charge densities as in Fig .3 are used. 5000 data points are obtained from calculations to plot the graph.*

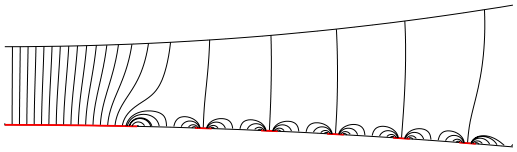

Figure 5. *Electric field lines for the same configuration as in Fig. 4. The bottom and top arcs show parts of the photoconductor and the development roller, respectively. The thick lines on the photoconductor surface represent images of a line and five dots. The field lines are drawn by starting at evenly distributed points on the photoconductor so that the density of the field lines are not proportional to the magnitude of the field.*

the drum and the roller which exerts on triboelectrifically charged toner. The exact calculation of the electrostatic field is not easy. One reason is that there is the large effect of charged toner on the field, which could be about as large as 30 percent of the surface charge on the photoconductor [1], which is ignored in our calculations. There are also influences of viscous force, adhesion force, friction, collisions between toner particles, etc. Any approximate inclusion of all the sources is very complex and becomes computationally intensive. Here we apply a simple model to capture the essence of the toner movement in the gap.

The total force which toner particles experience in the region between the drum and the roller can be divided into two groups. One is terms for the force which is applied to a toner particle if there exits only one particle in the development gap. The other is correction terms to the first group of terms from the existence of many toner particles. While one particle flies in the gap, the force sources are the electrostatic field and the viscosity of the air. The electric field calculated with the method described above will be used for the former and the Stokes term [9, 10] for the latter. When a particle contacts one of the surfaces, the image force and the Van der Waals force only are assumed to exist, which plays as the adhesion force.

The many-particle terms have to account for collisions between toner particles through mechanical and electrical interactions. These collisions occur irregularly in short time intervals. So in stead of considering exact particle collisions, many-particle interaction terms are simplified with a random force for the collisions. Specifically, random Gaussian forces will be used in the simulations. Then, the equation of motion for each toner particle in the gap for the development process becomes a Langevin-type equation [11],

$$m\frac{d\mathbf{x}}{dt} = q\mathbf{E} - 6\pi r\eta\mathbf{v} + \zeta(t)\,, \tag{7}$$

where m is the mass of a toner particle, q the toner charge, $\mathbf{E}$ the electrostatic field calculated from Eq. (3) and Eq. (4), $-6\pi r\eta\mathbf{v}$ the viscous force in the air with the viscosity of air η and the radius of the toner particle according to Stokes' law, and $\zeta(t)$ a random force with a Gaussian distribution. With Eq. (7) the many-particle process of image development between the drum and the roller is modeled as a collection of many single particle processes. The stochastic differential equation is solved numerically to obtain the trajectories of toner particles in the development process.

Simulation

The simulation begins with the preparations of a charge distribution on the photoconductor drum corresponding to image patterns to be developed, and a layer of charged toner on the development roller. The photoconductor has a charge distribution for an image consisting of a solid and a halftone below the solid. The surfaces of the drum and the roller move in opposite directions in the gap with an alternating square development bias applied between the drum and the roller. In the development process, particles start jumping at a certain point on the development roller and proceed through the gap as they keep jumping according to the equation of motions Eq. (7), until the particles settle on the drum surface.

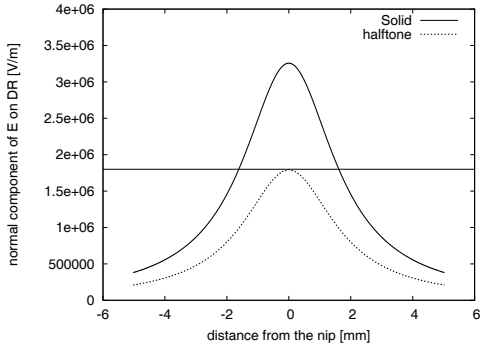

Figure 6. *The outward normal component of the electric field on the surface of the development roller for a solid image and a halftone image. The graph is plotted with 3000 data points. The horizontal line at the maximum value for the halftone is drawn for reference purpose.*

From the simulations it is observed that the region in which toner particles jump shifts for a solid image and a halftone image. This jumping region for halftones is narrower and closer to the position of the smallest gap than for solids. As toner particles on the development roller approach the development gap, the electrostatic force on the particles become stronger. When the outward normal component of the electrostatic force becomes greater than

the adhesion force which holds the particles onto the roller, the particles leave the surface of the roller. The reversed relationship between the electrostatic force and the adhesion force on the photoconductor drum holds when the toner jumping ends. The outward normal component of the electrostatic field on the development roller is shown in Fig. 6. One can see from the graph that there exists a length difference between the positions of a same outward normal component of the electric field for a solid and a halftone on the photoconductor. This causes the starting point of the toner jumping for halftones shifts to the deeper inside of the development gap compared to the case of solids. One can see the shift of the onset point of the toner jumping by comparing the two figures, Fig. 7 and Fig. 8, from the simulation data.

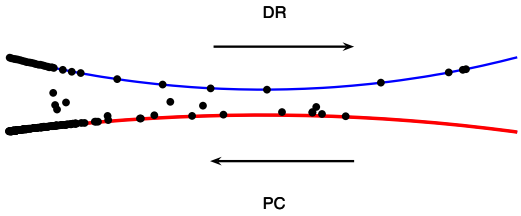

Figure 7. *Toner jumping in the development of a solid image. The onset of the jumping is seen in the left.*

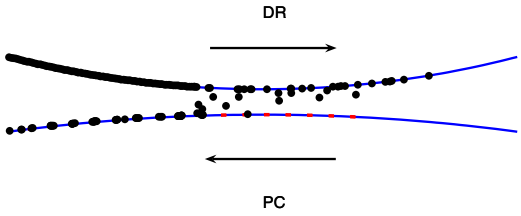

Figure 8. *Toner jumping in the development of a halftone image. The onset point of the jumping is moved toward the center of the gap compared to Fig. 7.*

The mechanism of the line deletion can be understood with this shift of the onset piont of the toner jumping. As the interface of the solid and the halftone enters the development gap, the starting point of the jumping shifts to the inner side of the gap. While this shifting occurs, the leading edge of the halftone on the photoconductor keeps moving away from the gap, but the toner does not start jump until the toner reach the starting point for halftone, when the surfaces of the drum and the roller move in opposite directions. Thus, there is not sufficient toner to be attracted to the leading edge of the halftone.

Summary

An image defect at an interface between a solid and a halftone was examined by numerical simulations of the toner movement between the photoconductor drum and the development roller in a two dimensional geometry. The occurrence of line deletion at the leading edge of a halftone image placed below a solid was analyzed for noncontact monocompoment systems with nonmagnetic toner in which the surfaces of the drum and the roller move in opposite directions. It was argued that the line deletion is due to the shift of the staring point of the toner jumping between the developments of the solid and the halftone.

Acknowledgments

The authors would like to thank H.C. Lee for his support during the work in the paper. We are also grateful to H.W. Bae, J.W Lee, J.W. Moon, Y.K. Shim, C.S. Yang, and M.N. You for helpful discussions.

References

[1] D.M. Pai and B.E. Springett, Review of Modern Physics, Vol. 65, pg. 163 (1993).

[2] L.B. Schein, *Electrophotography and Development Physics*, Springer-Verlag, New York (1998).

[3] J.G. Shaw, T. Retzlaff, IS&Ts NIP 15, pg.467 (1999).

[4] R.J. Meyer and A.T. Retzlaff, Jr., U.S. Patent 7,016,073 (2006).

[5] K.J. Binns, P.J. Lawrenson, C.W. Trowbridge, *The Analytical and Numerical Solution of Electric and Magnetic Fields*, John Wiley (1992).

[6] J. Yi, IS&Ts NIP 21, pg.586 (2005).

[7] J.D. Jackson, *Classical Electrodynamics*, 3rd Ed., Wiley, New York (1998).

[8] G. Dahlquist and A. Bjorck., *Numerical Methods*, Dover (2003).

[9] P.A. Baron and K. Willeke, *Aerosol Measurement: Principles, Techniques, and Applications*, Wiley-Interscience, New York (2005).

[10] T.L. Thourson, IEEE Transactions on Electron Devices, Vol. 19, pg. 495 (1972).

[11] S. Chandrasekhar, Review of Modern Physics, Vol. 15, pg. 1 (1943).

Author Biography

J. Yoo earned his Ph.D. in physics. Since he joined the digital printing division of Samsung Electronics in 2005, he has been involved in the development of non-magnetic monocomponent development systems.